Transition metal cluster ion chemistry

P. B. Armentrout

Department of Chemistry, University of California, Berkeley, CA 94720 USA

Abstract

The reactivity and thermochemistry of ionic metal atoms and clusters has been explored using guided ion beam mass spectrometry. With this apparatus, cross sections of ion-molecule reactions can be measured from thermal energies to hundreds of eV. Application to metal cluster chemistry demonstrates its utility for elucidating reaction dynamics and mechanisms and for determining cluster binding energies and ligand binding energies for both ionic and neutral species. Early results compare the largely unreactive atomic Mn^+ with the dimer Mn_2^+.

Introduction

In 1981, Smalley and co-workers developed a truly universal metal cluster source by vaporizing a metal sample using a laser and seeding this metal in a supersonic expansion of He.[1] In contrast to the oven based technologies which have seen eminent success with the alkali metals[2] and some coinage metals,[3] the laser vaporization technique provides a routine means of forming a cluster beam of any metal. Many groups are now exploring the spectroscopy, ionization potentials and chemistry of these neutral cluster beams.[4] One particularly desirable experimental feature which this source does not incorporate, however, is the ability to produce size-selected clusters. One experimental approach to producing a size-selected cluster beam is to study ionized clusters and use mass spectrometry to isolate the desired cluster size. Such an approach has been utilized by several groups,[5] including our own.[6,7]

In our work, we have examined the reactions of metal dimer ions and contrasted their behavior with that of the monomer ion. Our work differs from other approaches in that we examine the reactions of these ions over an extended kinetic energy range. This allows us to determine such quantities as the metal-metal binding energy, the binding energy of ligands, and absolute cross sections and branching ratios for reactions. In this report, we describe studies of Mn_2^+ reacting with Ar, O_2, CO and C_2H_6.

Experimental

The ion beam apparatus used in these experiments has been described previously.[8] The production of atomic and dimeric manganese ions is detailed below. The ions are extracted from the source, accelerated, and focused into a 60° magnetic sector for mass analysis. The mass selected ion beam is decelerated to a selected kinetic energy and focused into an octopole ion trap which is floated at the nominal ion energy. The octopole guides the ions through the collision chamber containing the reactant gas. The pressure of the gas in the gas cell, measured by an MKS Baratron capacitance manometer, is in the range of 0.2 to 1.0 mTorr. This is sufficiently low that reactions due to multiple ion-molecule collisions are improbable. The octopole ion guide utilizes rf electric fields to trap ions in the radial direction and thus allows efficient collection of all ionic products and transmitted reactant ions. These ions are extracted from the octopole, focused into a quadrupole mass filter for mass analysis, and detected using a scintillation ion counter and standard ion counting techniques. A DEC MINC computer system controls the reaction conditions and data collection.

Mn^+ ions are produced in a surface ionization (SI) source. Here, $MnCl_2$ is vaporized in an oven and directed at a rhenium filament which is resistively heated to 2200 K. The metal halide decomposes on this filament and metal ions are produced by surface ionization of the resulting metal atoms. If we presume that the metal reaches equilibrium at the filament temperature before desorption, the state distribution of the Mn^+ beam produced by SI should have a Maxwell-Boltzmann distribution such that 99.8% of the Mn^+ ions are in the ^7S ground state. Previous studies in our lab of Mn^+ indicate that this is quite accurate.[9]

As in our previously published reports[6,7] concerning Mn_2^+, this ion is produced by electron impact ionization and fragmentation of $Mn_2(CO)_{10}$. By keeping the electron energy close to the appearance potential of Mn_2^+ (18.8 eV[10]), the internal energy of the dimer ions is kept low (several tenths of an electron volt). Three variations of this source have been utilized in our laboratories. The first, used exclusively in references 6 and 7, is an in-line electron impact source. This source produces a reasonably intense beam of Mn_2^+ but suffers because the inlet for the $Mn_2(CO)_{10}$ precursor heats up and decomposes the precursor, primarily to $Mn(CO)_5$. Ionization of this radical produces large amounts of $Mn(CO)_2^+$ which is only one mass unit higher than Mn_2^+.[5] To avoid this problem, the second source uses an electron beam which crosses the effusive vapor beam. This results in less decomposition (and therefore, much less $Mn(CO)_2^+$ formation) and internally colder ions, as ascertained by collision induced decomposition. Details of this characterization are below. Reactions of Mn_2^+ with O_2, CO and C_2H_6 are performed with ions produced in this fashion. Finally, in a third source, we produce the dimer ions in a high pressure drift cell patterned after that described by Bowers and co-workers,[11] Here, Mn_2^+ is produced by electron impact of $Mn_2(CO)_{10}$ but at one end of a cell which also

contains a bath gas (usually N_2) at pressures of 0.1 to 1.0 Torr. The dimer ions undergo numerous collisions with the bath gas while drifting to the other end of the cell in a weak electric field. These collisions should serve to thermalize the dimer ions at the temperature of the gas cell, 300 K. After exiting the drift cell the ions are gently extracted and enter the ion beam focussing and mass selection region of the apparatus as described above. Characterization of this beam is again by collision induced dissociation studies discussed below.

Retarding field energy analysis is used to determine the nominal energy zero and distribution of the ion beam energy. This analysis is achieved by sweeping the DC bias of the octopole trap through the nominal ion energy zero. Because the reaction zone and this energy analysis region are physically the same, ambiguities in the analysis resulting from contact potentials, space charge effects and focussing aberrations are avoided. From the derivative of the retarding curve, the true ion beam energy zero can be measured within 0.1 eV lab. The ion beam energy distribution is found to have a typical FWHM of 1.0 eV lab. The effect of the thermal motion of the gas in the reaction cell contributes a much larger uncertainty to the collision energy. The resultant energy distribution effectively broadens any sharp features in the excitation function. Both this effect and the ion beam energy distribution are taken into account when analyzing the experimental results.[12]

Reaction cross-sections, σ, are calculated using equation 1 which

$$I_r = (I_r + I_p) \exp(-n\sigma l) \tag{1}$$

relates the effective length of the interaction region, l (= 8.6 cm), and the number density of the target gas, n, to the measured intensities of the transmitted reactant ions and product ions, I_r and I_p. Individual product cross sections are calculated using equation 2. The largest

$$\sigma_i = \sigma \cdot I_i / \Sigma I_i \tag{2}$$

contribution to the uncertainty of our measurement of absolute cross sections results from uncertainties in the target gas density and effective cell length. We estimate these errors to be ±20%.

Results and Discussion

Collision induced dissociation

In our initial report[6] on the collision induced dissociation (CID) of Mn_2^+, reaction 3, we found that

$$Mn_2^+ + Ar \rightarrow Mn^+ + Mn + Ar \tag{3}$$

the kinetic energy threshold for CID depended strongly on the electron energy (Ee) used to form the dimer ion. This effect is clearly due to the production of internally excited ions which therefore require less kinetic energy to dissociate. At the lowest Ee which still produced a usable beam of Mn_2^+, ~18 eV, the kinetic energy threshold for CID was determined to be 0.85 ± 0.2 eV (20 ± 4 kcal/mol). We noted that this is strictly a lower limit to the true bond dissociation energy of Mn_2^+, $D°(Mn_2^+)$, but within our abilities to produce "cold" ions, we believed it to be fairly accurate.

Recently, Jarrold, Illies and Bowers[13] measured the bond energy of Mn_2^+ by photodissociation. In this experiment, the ions need not be produced without internal excitation since the kinetic energy release is directly measured. Unless there is a systematic problem with interpreting this data (e.g., dissociation from excited states having a much larger extinction coefficient or dissociation from an excited state of Mn_2^+ to excited atomic states), the photodissociation measurement rather unambiguously determines $D°(Mn_2^+) \geq 1.39$ eV (32 kcal/mol). The discrepancy with our value almost certainly lies in our ability to produce dimer ions with little internal excitation. The fact that despite our best efforts we apparently retained about 0.5 eV of excitation may indicate that there are many low lying electronically excited states which are easily populated by electron impact and which do not radiatively relax. Alternatively, if in the fragmentation-ionization of $Mn_2(CO)_{10}$, the CO molecules fall off rapidly compared with the relaxation of the metal-metal bond, then electron impact could produce vibrationally excited Mn_2^+ even at threshold.

To test our ability to produce a "cold" beam of ions, Mn_2^+ was produced in two different sources described above: a crossed electron beam source and a high pressure drift cell designed to produce thermalized ions. The results for CID of Mn_2^+ ions produced using the crossed electron beam source are shown in Figure 1. The means of interpreting the data have been detailed previously. The curve shown is described by equation 4 where E is the relative translational energy, E_{int} is the

$$\sigma(E) \propto (E + E_{int} - D°)^n / E \tag{4}$$

internal energy of the system, D° is the bond energy of the dissociating molecule, and n is found to be ~2. The translational energy threshold, $D°-E_{int}$, is found to be 1.1 ± 0.2 eV. Compared with the value determined by photodissociation, ≥1.39 eV, this indicates that there is still a couple of tenths of an electron volt of internal excitation. While the ions are certainly not "cold" in a spectroscopic sense, the internal excitation is reasonably under control. Very similar results are also obtained with the high pressure drift cell source. It is somewhat mystifying that this residual excitation cannot be eliminated by any means.

Reaction with O_2

The reactivity of Mn^+ and Mn_2^+ with O_2 differs appreciably. Figure 2 shows the cross section for reaction 5 and reactions

$$Mn^+ + O_2 \rightarrow MnO^+ + O - 2.3 \text{ eV} \quad (5)$$

6-12. The thermochemistry for these reactions comes from Table 1.

$$Mn_2^+ + O_2 \rightarrow Mn_2O^+ + O + 0.6 \text{ eV} \quad (6)$$

$$\rightarrow Mn^+ + MnO_2 + 3.0 \text{ eV} \quad (7)$$

$$\rightarrow Mn^+ + Mn + O_2 - 1.4 \text{ eV} \quad (8)$$

$$\rightarrow Mn^+ + MnO + O - 2.8 \text{ eV} \quad (9)$$

$$\rightarrow Mn^+ + Mn + 2O - 6.5 \text{ eV} \quad (10)$$

$$\rightarrow MnO^+ + MnO - \sim 0 \text{ eV} \quad (11)$$

$$\rightarrow MnO^+ + Mn + O - 3.7 \text{ eV} \quad (12)$$

Below 5 eV, the data for reaction 5 is in good agreement with a previous study of this reaction while above 5 eV, the cross section measured here exceeds that previously reported.[14] In the data for Mn_2^+, the results of Fig. 2 are in good agreement with a previously published brief account[7] below 3 eV. Above 3 eV, however, the data shown in Fig. 2 differs appreciably from the previous data. These discrepancies are due to instrumental improvements made in the collection of product ions.

It is obvious that the dimer ion is much more reactive than the atomic ion. The latter has only one reaction channel which is substantially endothermic and reaches a maximum of only 1×10^{-16} cm^2 at about 5 eV. Detailed analysis of this excitation function yields a threshold energy consistent with a MnO^+ bond energy of 2.80 ± 0.2 eV.[15] In contrast, several reaction channels exist for reaction of Mn_2^+. While the fact that there are more atoms in this system makes this an expected result, the fact that reactions 6 and 7 are exothermic is not expected. In fact, observation of reaction 6, in which the strong O_2 bond (D = 5.12 eV) is broken while the relatively weak Mn_2^+ bond (D = 1.4 eV) is retained, is quite a surprising result. Reaction 7, the only exothermic pathway for producing Mn^+, involves extensive rearrangement of the reactants to form the manganese dioxide product. Reaction 11, an apparent four center exchange process, is very close to thermoneutral. Reaction 8, the CID process, is obvious as the rise in the Mn^+ cross section beginning in the vicinity of 1.4 eV. Similarly, reaction 12 is indicated by the rise in the cross section for formation of MnO^+ beginning at 3.7 eV. Reaction 9, a high energy pathway to form Mn^+, is not observed directly due to the size of the Mn^+ cross section. The fact that it occurs is evidenced by the decrease in the cross section for Mn_2O^+ at the thermodynamic limit for this process. Likewise, reaction 10 can be seen as the threshold for the decrease in the cross section for MnO^+. It is important to point out that the ability to determine the multitude of reaction pathways in the $Mn_2^+ + O_2$ system is a direct result of measuring the kinetic energy dependence of the cross sections.

Reaction with CO

Reaction of Mn^+ with CO results in the production of $MnO^+ + C$ and $MnC^+ + O$. Both reactions are endothermic. Their threshold behavior has been analyzed to yield the bond energy for MnC^+ of 2.2 ± 0.6 eV.[15] The predominant reaction of Mn_2^+ with CO is the CID process which has a threshold consistent with the CID results above and reaches a cross section of about 8×10^{-16} cm^2. This is certainly reasonable considering that CO has a bond energy of 11.14 eV, 8 times larger than that of Mn_2^+. It is then surprising that any chemistry at all is observed; however, Fig. 3 shows that at high energies the chemistry is rather extensive. Again we observe retention of the metal dimer accompanying cleavage of the reactant neutral to form both Mn_2O^+ and Mn_2C^+. Analysis of the thresholds for these reactions permits the tentative assignment of the thermochemistry for these species listed in Table 1. Because of the internal energy of the Mn_2^+, these bond energies are best viewed as upper limits but are probably reasonably accurate within the listed uncertainties. Reaction of Mn_2^+ with CO also produces the ions MnC^+ and MnO^+. Based on the known thermochemistry of these species, their formation at the observed kinetic energies, Fig. 3, must be accompanied by production of the bound neutral products, MnO and MnC, respectively. By examining the threshold behavior of these reaction channels, we can measure the bond energies of these neutral species, Table 1. The value derived for D(MnO) is in reasonably good agreement with the literature value, 3.7 ± 0.17 eV.[16]

Reaction with C_2H_6

Figure 4 shows the results for reaction of Mn_2^+ with ethane. The CID channel, formation of Mn^+, is not shown but is comparable in magnitude to the cross section for Mn_2H^+ and has a lower threshold. As in the other reaction systems, there are prominent product channels in which the metal dimer is retained, Mn_2H^+ and $Mn_2CH_3^+$. Not shown are minor channels, $Mn_2CH_2^+$ and Mn_2CH^+, for which this is also true. The threshold behavior of the various reactions has been analyzed and the thermochemistry for Mn_2H^+, $Mn_2CH_3^+$, MnH and $MnCH_3$

has been derived, Table 1. Studies of Mn^+ reacting with H_2 and ethane provide data on MnH^+ and $MnCH_3^+$. These results demonstrate that reasonably complex systems of real chemical interest can be examined and analyzed to yield extensive thermochemical and kinetic data.

Thermochemistry

The thermochemical results of these studies are summarized in Table 1. Several interesting comparisons can be made

Table 1: Bond Energies of Manganese Species[a]

L	D(Mn-L)	$D(Mn^+-L)$	$D(Mn_2^+-L)$
H	<1.4	2.06 (0.15)	2.1 (0.3)
CH_3	<1.3	2.2 (0.3)	2.4 (0.3)
C	2.5 (0.4)	2.2 (0.6)	4.5 (0.4)
O	3.8 (0.2)	2.8 (0.2)	5.7 (0.4)

[a] All values in eV. Uncertainties in parentheses. From this work and related studies (refs. 9 and 15).

between the neutral and ionic atomic Mn species and also between the monomeric and dimeric ion species. First, it can be seen that the values for $D(Mn^+-L)$ are all nearly the same. This may be the result of the electron configuration of Mn^+ which is $4s3d^5$. Since the half-filled 3d shell is very stable, it seems likely that only the 4s electron is accessible for bonding. If this is the case, then Mn^+ will tend to form only a single bond with other species. The fact that MnO^+ is slightly stronger may be due to ionic components of the bonding or to some covalent double bond character. Contrast this behavior with the neutral MnL species. Now, the ligands which can only form single bonds, i.e., H and methyl, have weaker bonds with Mn than with Mn^+ while those ligands which can form multiple bonds, i.e., C and O, bind more strongly to Mn. Since the electron configuration of Mn is $4s^23d^5$, these results can be rationalized by assuming that in forming a single bond, the energy lost by disrupting the filled 4s shell of Mn is high. Therefore, the bonding to Mn is weaker than to Mn^+ where the 4s orbital is only half-filled. However, while Mn^+ cannot form multiple bonds due to the inaccessibility of the 3d electrons, neutral Mn can utilize both 4s electrons in the bonding process.

Now, consider the monomeric and dimeric ion species. Note that the singly bonding ligands, H and CH_3, have comparable bond energies for Mn^+ and Mn_2^+. The multiple bonding ligands, C and O, however, have much stronger bonds with the dimer ion than with the atomic ion. This seems to imply that the carbon and oxygen atoms interact strongly with both metal atoms. Unfortunately, these experiments cannot provide any structural information to confirm the nature of this strong interaction.

Conclusion

While our experiments to date have included only a comparison of dimer and monomer ions, it is clear from these studies that similar information can be obtained with larger clusters. Indeed, if progress is to be made in using gas phase clusters as models for catalytic chemistry, this type of quantitative information is absolutely necessary and one of the primary motivations of such comparisons. Ongoing work in our laboratories is directed at producing larger clusters by several techniques to carry on such studies. Because it is critical to have thermalized clusters for these thermochemical studies, all these approaches incorporate supersonic expansion for cooling. Vaporization techniques include the use of a high repetition rate Cu vapor laser, particle beam sputtering and a DC rare gas arc.

Acknowledgements

The author wishes to thank S. K. Loh and D. Hales who performed most of the experiments discussed in this paper. This work is supported by the Army Research Office, DAAG29-84-0077 and DAAG29-85-K0181. We also gratefully acknowledge contributions from Exxon Corporation.

References

1. T. G. Dietz, M. A. Duncan, D. E. Powers, and R. E. Smalley, J. Chem. Phys. 74, 6511-6512 (1981).
2. See (for example A. Herrmann, S. Leutwyler, E. Schumacher, and L. Woste, Helv. Chim. Acta, 61, 453-487 (1978); M. M. Kappes, R. W. Kunz, and E. Schumacher, Chem. Phys. Lett. 91, 413 (1982); W. A. Saunders, K. Clemenger, W. A. deHeer and W. D. Knight, Phys. Rev. B 32, 1366 (1985); J. L. Gole, G. J. Green, S. A. Pace, and D. R. Preuss, ibid., 76, 2247 (1982).
3. D. R. Preuss, S. A. Pace, and J. L. Gole, J. Chem. Phys. 71, 3553 (1979); B. G. DeBoer and G. D. Stein, Surf. Sci. 106, 84 (1981); A. E. T. Kuiper, G. E. Thomas, and W. J. Schouten, J. Crystal Growth, 51, 17 (1981).

4. See for example (a) P. R. R. Langridge-Smith, M. D. Morse, G. P. Hansen, and R. E. Smalley, J. Chem. Phys. 80, 593 (1984); M. D. Morse, M. E. Geusic, J. R. Heath, and R. E. Smalley, J. Chem. Phys. 83, 2293 (1985). (b) S. J. Riley, E. K. Parks, L. G. Pobo, and S. Wexler, J. Chem. Phys. 79, 2577 (1983); S. C. Richtsmeier, E. K. Parks, K. Liu, L. G. Pobo, and S. J. Riley, J. Chem. Phys. 82, 3659 (1985). (c) E. A. Rohlfing, D. M. Cox, and A. Kaldor, Chem. Phys. Lett. 99, 161 (1983); D. J. Trevor, R. L. Whetten, D. M. Cox, and A. Kaldor, J. Am. Chem. Soc. 107, 518 (1985); R. L. Whetten, D. M. Cox, D. J. Trevor, and A. Kaldor, Phys. Rev. Lett. 54, 1494 (1985).
5. (a) R. B. Freas and D. P. Ridge, J. Am. Chem. Soc. 102, 7129 (1980); D. P. Ridge, "Ion Cyclotron Resonance Spectrometry," Ed. H. Hartman and K. P. Wanczek (Springer-Verlag, New York, 1982). (b) B. S. Freiser, Talanta 32, 697 (1985); D. B. Jacobson and B. S. Freiser, J. Am. Chem. Soc. 107, 1581 (1985). (c) L. S. Zheng, P. J. Brucat, C. L. Pettiette, S. Yang, and R. E. Smalley, J. Chem. Phys. 83, 4273 (1985). (d) L. A. Bloomfield, M. E. Geusic, R. R. Freeman, and W. L. Brown, Chem. Phys. Lett. 1221, 33 (1985). (e) G. Delacretaz, P. Fayet, and L. Woste, Ber. Bunsenges Phys. Chem. 88, 284 (1984).
6. K. Ervin, S. K. Loh, N. Aristov, and P. B. Armentrout, J. Phys. Chem. 87, 3593-3596 (1983).
7. P. B. Armentrout, S. K. Loh, and K. M. Ervin, J. Am. Chem. Soc. 106, 1161-1163 (1984).
8. K. M. Ervin and P. B. Armentrout, J. Chem. Phys. 83, 166-189 (1985).
9. J. L. Elkind and P. B. Armentrout, J. Chem. Phys. submitted for publication.
10. R. E. Winters and R. W. Kiser, J. Phys. Chem. 69, 1618 (1965).
11. P. A. M. Van Koppen, P. R. Kemper, A. J. Illies, and M. T. Bowers, Int. J. Mass Spectrom. Ion Proc. 54, 263-282 (1983).
12. C. Lifshitz, R. L. C. Wu, T. O. Tiernan, and D. T. Terwilliger, J. Chem. Phys. 68, 247 (1978); P. J. Chantry, ibid., 55, 2746 (1971).
13. M. F. Jarrold, A. J. Illies, and M. T. Bowers, private communication.
14. P. B. Armentrout, L. F. Halle, and J. L. Beauchamp, J. Chem. Phys. 76, 2449 (1982).
15. S. K. Loh, D. Hales, K. M. Ervin, and P. B. Armentrout, work in progress.
16. C. J. Cheetam and R. F. Barrow, Adv. High Temp. Chem. 1, 7 (1967).

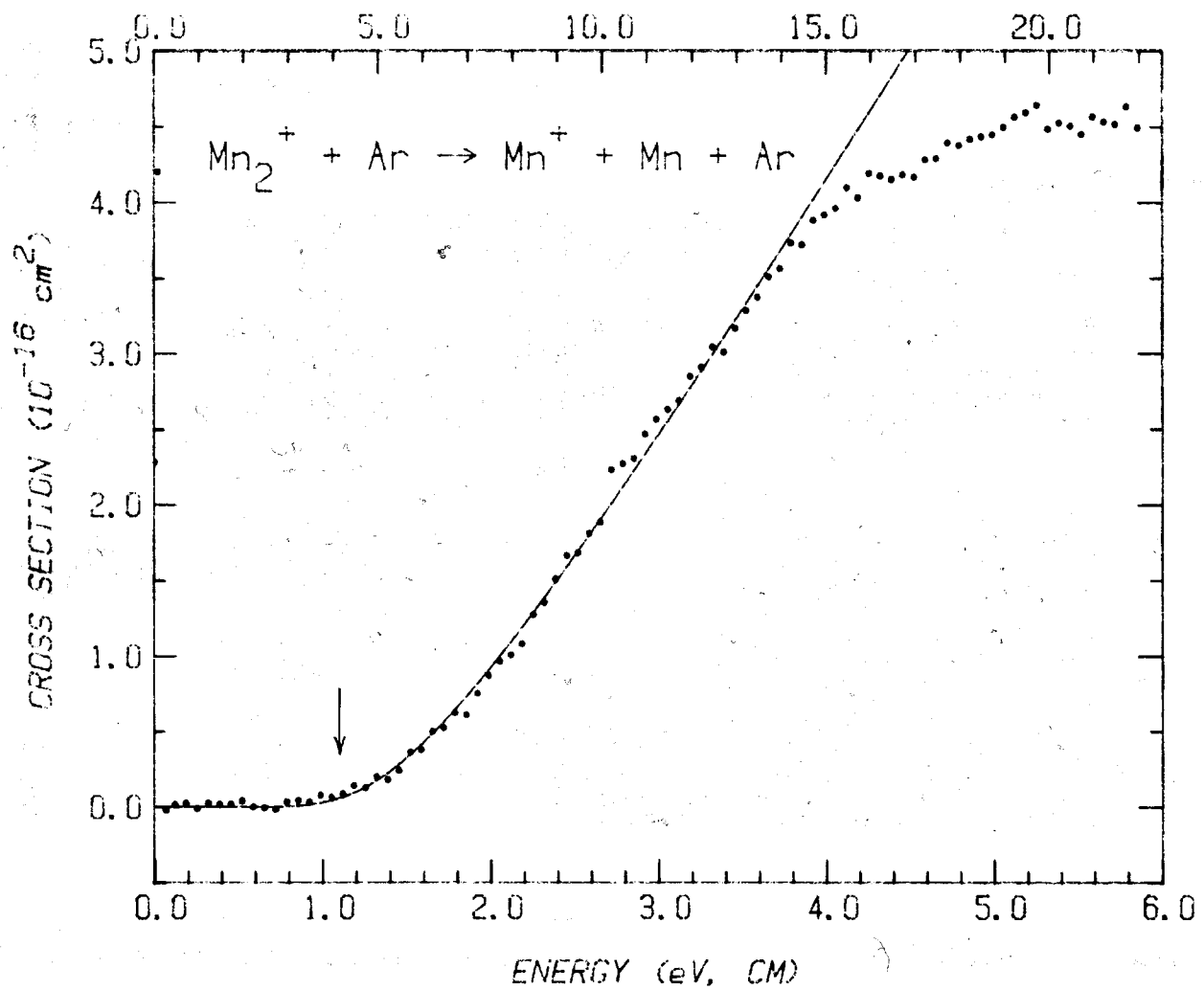

Figure 1. Collision induced dissociation cross section for reaction 3 as a function of relative kinetic energy (lower scale) and laboratory energy (upper scale). The line is the theoretical fit to the data described in the text. The arrow indicates the threshold energy determined from this analysis.

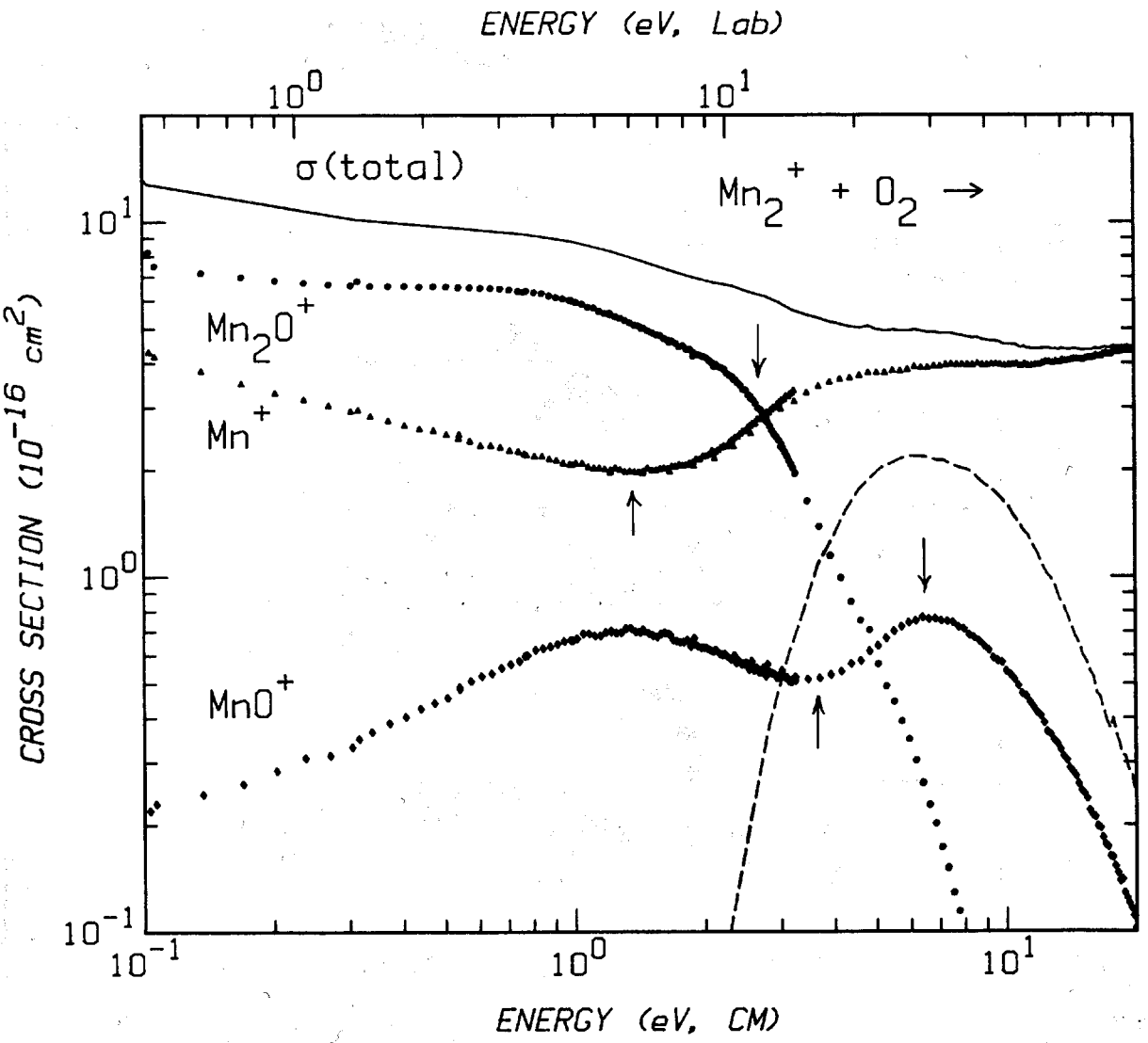

Figure 2. Cross section for reaction of Mn_2^+ with O_2 as a function of relative kinetic energy (lower scale) and laboratory energy (upper scale). Arrows indicate the threshold energies for reactions 8(1.4 eV), 9(2.8 eV), 10(6.5 eV), and 12(3.7 eV). The dashed line shows the cross section for atomic Mn^+ with O_2, reaction 5, on the same relative kinetic energy scale.

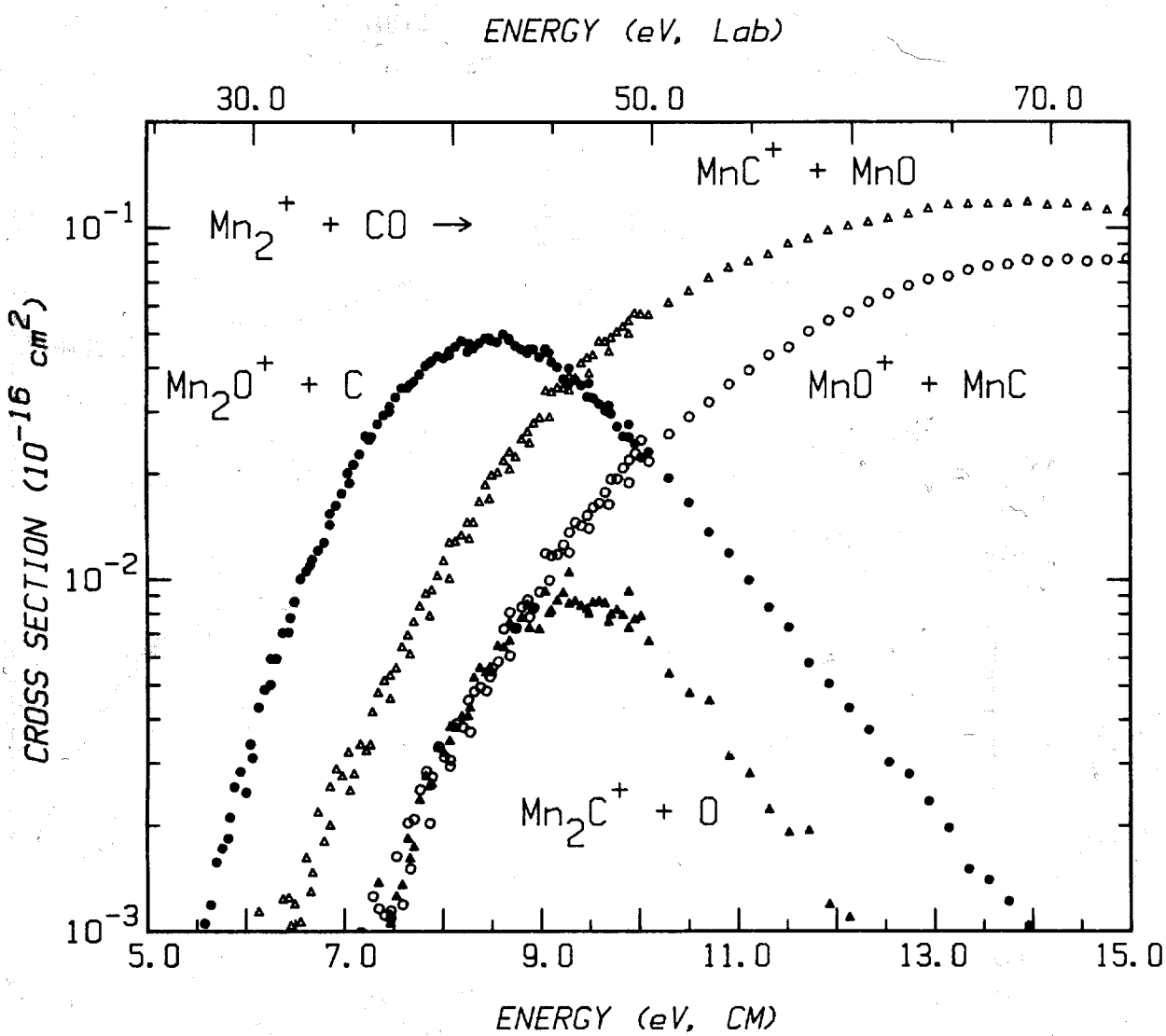

Figure 3. Cross section for reaction of Mn_2^+ with CO as a function of relative kinetic energy (lower scale) and laboratory energy (upper scale). The major product channel, Mn^+, is not shown, see text.

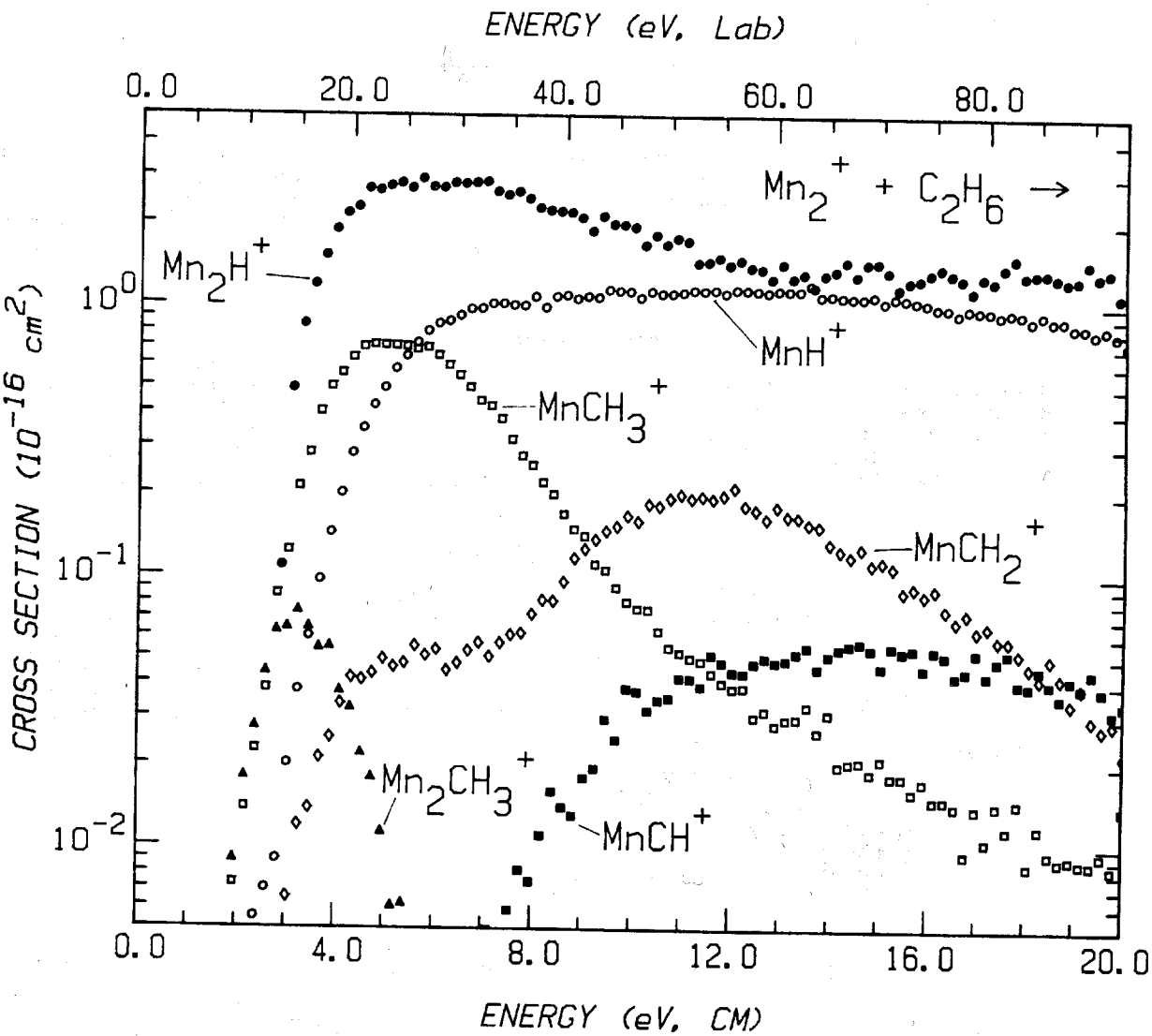

Figure 4. Cross section for reaction of Mn_2^+ with ethane as a function of relative kinetic energy (lower scale) and laboratory energy (upper scale).[2] Several minor channels are not shown nor is production of Mn^+, see text.